Donor-dependent Fecal Microbiota Transplantation Efficacy Against Necrotizing Enterocolitis in Preterm Pigs

Yan Hui
University of Copenhagen: Kobenhavns Universitet https://orcid.org/0000-0002-2388-131X
Gisle Alberg Vestergaard
Danmarks Tekniske Universitet
Ling Deng
University of Copenhagen: Kobenhavns Universitet
Witold Piotr Kot
University of Copenhagen: Kobenhavns Universitet
Thomas Thymann
University of Copenhagen: Kobenhavns Universitet
Anders Brunse
University of Copenhagen: Kobenhavns Universitet
Dennis Sandris Nielsen (dn@food.ku.dk)
University of Copenhagen https://orcid.org/0000-0001-8121-1114

Research

Keywords: fecal microbiota transplantation, necrotizing enterocolitis, preterm neonates, high-throughput sequencing

Posted Date: December 3rd, 2020

DOI: https://doi.org/10.21203/rs.3.rs-117422/v1

Abstract

Background

Fecal microbiota transplantation (FMT) has shown high cure rates against recurrent *Clostridioides difficile* infection regardless of donor microbiota characteristics, whereas the clinical response of FMT in inflammatory bowel disease appears to be donor-dependent. We recently showed that FMT from healthy suckling piglet donors to newborn preterm piglets decreased the risk of necrotizing enterocolitis (NEC), a serious gastrointestinal disease of preterm infants, but could not replicate this finding in a follow-up study using phenotypically similar donors. This gave us the opportunity to directly investigate the microbiota dynamics of clinically efficient FMT. In this experiment, preterm piglets (n=38) were randomly allocated to receive control saline or FMT from inferior (FMT1) or superior donors (FMT2) by rectal administration. All animals were fed infant formula for four days to induce NEC-like lesions before necropsy and gut pathological evaluation. Donor and recipient colonic microbiotas were analyzed by 16S rRNA gene amplicon sequencing and shotgun metagenomics.

Results

Although the two donor microbiotas closely resembled one another, only FMT2 recipients had improved body growth and lower intestinal permeability relative to control, and were protected against NEC. Both FMT groups had shifted colon microbiota composition relative to CON, with increased lactobacilli relative abundance, but FMT2 recipients had a higher lactobacilli abundance relative to FMT1. *Limosilactobacillus reuteri* and *Lactobacillus crispatus* strains of FMT recipients showed high phylogenetic similarity with their respective donors, indicating successful engraftment. Further, NEC severity was positively associated with *Clostridoides difficile*, *Clostridium perfringens* and *Enterococcus faecium* abundance, while *Lmb. reuteri* and *Lb. crispatus* negatively correlated with diarrhea severity. Genome-resolved analysis indicated a higher gut replication rate of lactobacilli in FMT2 recipients, and identified specific glycosaminoglycan-degrading *Bacteroides* in the superior donor.

Conclusions

FMT efficacy against NEC is donor-dependent, and introduced lactobacilli manifest strain-level differences with respect to colonizing recipients. Using shotgun metagenomics, we traced the engrafted strains back from donors and identified donor-specific microbes of potential importance. This may accelerate our understanding of optimal donor selection for clinical FMT.

Background

Necrotizing enterocolitis (NEC) is a devastating intestinal inflammation primarily affecting infants born preterm with an incidence of up to 7% [1, 2]. First reported in the early 1800s [3], NEC has been intensively investigated but the underlying etiology is only partially understood [1]. In the neonatal period, the combination of impaired host antimicrobial defense mechanisms and gut dysbiosis (presence of

opportunistic pathogens and absence of commensals) might initiate a lethal hyperinflammatory reaction in the gut mucosa [4, 5]. The preterm gut microbiome (GM) is often dominated by *Enterococcaceae* and *Enterobacteriaceae* [6, 7, 8] and large-scale metagenomic studies have shown increased *Proteobacteria* [9] and bacterial replication rates of *Enterobacteriaceae* prior to NEC incidence [10]. Although no single microbe has consistently been reported as a direct cause, accumulated evidence strongly indicates that gut microbial dysbiosis is an important risk factor for NEC.

Indeed, numerous GM-targeted interventions have been tested to prevent NEC. Examples include the use of prophylactic peroral aminoglycoside which reduces NEC incidence but is not considered feasible due to the risk of antimicrobial resistance and other potential side effects [11]. Prophylactic probiotic supplementation appears to reduce NEC incidence with few side effects [12] and is routinely used in preterm infants, although the optimal combination of bacterial strains, dose and timing is unknown. Regardless, the NEC incidence rate of 5–10% for very-low-birth-weight infants as well as the 10–30% mortality rate has not improved significantly the past 20 years [2, 13].

Through restoring the microbial diversity in the gastrointestinal tract, fecal microbiota transplantation (FMT) has been widely and effectively used to treat recurrent *Clostridoides difficile* infection (rCDI), showing high cure rates independent of specific donors [14, 15]. However, FMT therapies targeting inflammatory bowel disease (IBD) have shown discrepant clinical efficacy associated with the fecal donors [16, 17, 18, 19]. Previously we have shown that rectal FMT can significantly reduce NEC incidence in preterm piglets while modulating the GM and host immune response with reduced mucosal proinflammatory *TLR4* signaling [20]. Accordingly, using comparable donor material we failed to reproduce the NEC-reducing effect of FMT in a follow-up experiment. This led us to hypothesize that NEC prevention by FMT depends on the donor microbiome characteristics. Formula-fed preterm piglets display most clinical and pathological features of human NEC from feeding intolerance and bloated abdomen to intestinal necrosis and peritonitis [21]. This makes preterm piglets an appropriate model for microbial interventions in preterm neonates. In a controlled experiment, we randomly allocated preterm pigs to receive FMT from either inferior or superior fecal donors. To compare gut microbial responses and investigate engraftment patterns, we characterized the gut microbiota of donors and recipients using 16S rRNA gene amplicon sequencing and shotgun metagenomics.

Methods

Animals and Experimental Setup

Experimental animal procedures were approved by the Danish Animal Experiments Inspectorate (2014-15-0201-00418). Thirty-eight crossbred piglets (Landrace × Yorkshire × Duroc) from two sows were delivered at 90% gestion (106 days) and fitted with oro-gastric feeding tube and arterial catheter inserted through the transected umbilical cord. Animals were housed in heated incubators (37–38 °C) with oxygen supply as previously outlined [22]. To account for the lack of transplacental immunoglobulin transfer, passive immunization was provided by arterial infusion of maternal plasma (16 ml/kg) and followed by

parenteral nutrient supplementation (2–4 ml/kg/h, Kabiven, Vamin, Fresenius-Kabi, Bad Homburg, Germany). Increasing volumes of infant formula (3–12 ml/kg/3 h) was administered in the feeding tube from birth to day 5.

Fecal microbiota transplantation

Two donor solutions were prepared from pooled colon content of four 10-day-old healthy pigs (Landrace × Yorkshire × Duroc) from two different herds (Fig. 1). The donor pigs were euthanized and colon content collected, pooled, diluted 1:1 in 20% sterile glycerol and stored at -80 °C as previously described [20]. Before use, donor feces were thawed and diluted to a working concentration of 0.05 g/ml after filtration through a 70-μm cell strainer to remove macroscopic debris. Animals were stratified by gender and birth weight and randomly allocated to receive rectal administration of 0.5 ml working fecal solution from Donor 1 (FMT1, n = 13), Donor 2 (FMT2, n = 13) or sterile physiological saline (CON, n = 12). The FMT was administered twice on days 1 and 2 (one dose pr. day).

Clinical evaluation and tissue collection

Animals were monitored by experienced personnel throughout the experiment, and daily weights and stool patterns recorded. Any animal with signs of systemic illness (e.g. lethargy, respiratory distress, hypoperfusion) was immediately euthanized. On day 5, remaining animals were euthanized with a lethal dose of intracardiac barbiturate under deep anesthesia. Three hours before scheduled euthanasia, animals received a 15 ml/kg oro-gastric bolus of lactulose and mannitol (5/5% w/v) to measure intestinal permeability by urinary recovery. After exposing the abdominal cavity, urine was collected by bladder puncture for lactulose and mannitol measurement [23]. Gross pathological evaluation of stomach, small intestine and colon was performed according to a validated six-grade NEC scoring system [20]. NEC was defined as pathology grade 4 (extensive hemorrhage) in at least one gastrointestinal segment, and both incidence and severity (mean score across all three gut segments) were reported. Small intestine and colon tissues were immersion fixed in 4% paraformaldehyde and paraffin-embedded for histological assessment of bacterial adhesion by fluorescence *in situ* hybridization (FISH) goblet cell fraction determination by Alcian Blue-Periodic acid-Schiff (AB-PAS) staining, and T-cell and myeloid cell areas by CD3 and myeloperoxidase (MPO) immune staining, respectively [20]. Brush-border enzyme activities were determined in tissue samples from the proximal, mid and distal small intestine as previously described [23]. Colon content was collected and snap-frozen for 16S rRNA gene amplicon sequencing and shotgun metagenomics.

DNA extraction and high-throughput sequencing

Total DNA was extracted from colon content using Bead-Beat Micro AX Gravity Kit (A&A, Gdynia, Poland) according to the manufacturer's instructions. The V3 region of 16S rRNA gene was amplified for prokaryotic community characterization by NextSeq 150 bp pair-end sequencing (Illumina, San Diego, CA, USA) as previously reported [24]. Technical replicates of donors were sequenced for amplicon sequencing. For broader profiling, 150 bp pair-end metagenomic shotgun sequencing on Illumina Novaseq 6000 was conducted after PCR-free library preparation with KAPA HyperPrep Kit (KAPA

Biosystems). The shotgun sequencing was carried out by a commercial sequencing service provider (Admera Health, South Plainfield, NJ, USA).

Bioinformatic processing of 16S rRNA gene amplicon sequencing data

Amplicon sequencing data analysis was carried out as previously described [25]. In short, raw sequencing reads were merged and trimmed to construct zero-radius operational taxonomic units (zOTUs) after removing chimeras [26]. The Greengenes database (v13.8) was used as annotation reference. Post analysis and visualization were performed using Phyloseq [27]. Raw zOTU-data was rarefied at 11000 counts to calculate Shannon diversity index and beta-diversity metrics (weighted and unweighted UniFrac distance metrics). For both amplicon and shotgun profiling, the genus-level taxonomic names of taxa previously belonging to the genus *Lactobacillus* were updated manually according to the recent announcement and the term “lactobacilli” was used in this paper to represent members of lactic acid bacteria belonging to the *Lactobacillus* genus as it was defined until the publication of [28].

Bioinformatic processing for shotgun metagenomics

The bioinformatic workflow for shotgun metagenomics and integration with clinical data followed the strategy illustrated in Figure S1 (Additional file), and GNU-parallel was used to execute jobs in parallel [29]. Quality control of raw reads utilized Read_qc module within metaWRAP [30]. PhiX174 control and host genome (*Sus scrofa* 11.1, GCA_000003025.6) was removed using BMTagger and followed by Trim Galore for adapter and quality trimming, resulting in total 317 Gb clean data with a mean depth of 7.9 Gb per sample. The taxonomic profiling was done with Kaiju [31] through protein-translated search against all prokaryotic and viral proteins in the NCBI_nr database plus microbial eukaryotic proteins (2019.6) under the default settings. Kaiju-based results were summarized at phylum, genus and species level to calculate the respective diversity index and GM abundance, and the unclassified reads (Mean: 4.4%, Min: 0.8%, Max: 20.2%) were removed. The abundance matrix was normalized with Hellinger’s transformation before calculating the binary Jaccard and Bray Curtis distance metrics. For *de novo* assembly, each sample was individually assembled with metaWRAP [30] Assembly module under –use-metaspades mode [32] and then all the reads were co-assembled under –use-megahit mode.

Metagenome functional annotation

The individually- and co-assembled contigs were concatenated together for open reading frames (ORFs) prediction with MetaGeneMark [33] (v3.38), followed by clustering with Linclust [34] under the criteria of 95% identity and overlap > 90% (–min-seq-id 0.95, -c 0.9) to construct a non-redundant gene catalogue. Short ORFs with length less than 100 bp were removed with seqkit [35]. Remaining ORFs were annotated against the KEGG gene database (2019.05.15) using GhostKOALA [36]. Clean reads were mapped back to the non-redundant gene set using bwa [37] and samtools [38] to calculate gene abundance. Reads with mapping quality better than 30 were kept and each pair of reads mapped to the same gene counted once.

Prokaryotic MAGs reconstruction and MAG-level analysis

To avoid fragmented assemblies for similar strains [39], individually assembled long scaffolds (> 2000 bp) were binned with maxbin2, concoct and metabat2 in metaWRAP [30] Binning module. Putative bins from each sample were dereplicated using dRep [40] (-comp 50 -con 5 –sa 0.99) to generate a medium quality bin set (completeness > 50% and contamination < 5%) for each binner. Two-step bin refinement was adopted with the Bin_refinement module to combine results from the three binners and another deep-learning-based binner Vamb (v2.1) [41]. For Vamb, genomic bins of more than 200,000 base pairs were included. This subject-specific binning strategy extracted more complete bins compared with direct binning on co-assemblies (Additional file: Figure S2).

The abundance of refined bins were determined by the Quant_bins module in metaWRAP [30]. The ORFs of refined MAGs were called using prodigal [42] under metagenomic mode (-p meta) and annotated by KEGG gene database using GhostKOALA [36]. The breadth of coverage (covered percentage of genomic size) of MAGs in each sample was estimated by coverm [43]. The MAGs with a breadth of coverage > 50% were considered “detected” in one sample. Based on the breadth of coverage information, MAGs were grouped as “Donor1-specific”, “Donor2-specific”, “Donor shared” and “Recipients specific”. The linkage and taxonomy of the MAGs were assessed by MAGpy [44] to integrate results from PhyloPhlAn, Checkm and blast against UniProt database.

To estimate the bacterial replication rate (as a surrogate measure of growth rate), the generated MAGs were first dereplicated using dRep [39] under 99% clustering threshold (the ANImf algorithm) and 25% minimum coverage overlap, and iRep [45] values were calculated based on the mapped reads against the representative MAGs. Default settings for iRep were adopted.

Strain tracking of Lactobacillus crispatus and Limosilactobacillus reuteri

Lb. crispatus and *Lmb. reuteri* strains from the 2 donors were tracked using clade-specific marker genes from StrainPhlAn [46] and functional gene alignment with PanPhlAn [47]. The reference assembly of *Lb. crispatus* and *Lmb. reuteri* on NCBI Refseq were downloaded to generate the respective gene database for PanPhlAn [47]. Genes on assemblies were called using Prokka [48] and annotated against KEGG gene database using GhostKOALA [36].

Statistics

All statistical analysis was performed using R version 3.6.3, and the results were visualized using R package ggplot2 [49] unless stated otherwise. The phenotypic data except NEC incidence (Fisher’s exact test) was analyzed by linear mixed models with treatment group as a fixed factor and sow as a random factor (lmer function in R package lme4 [50]), and Tukey’s post-hoc test was used for pairwise comparison (lsmeans function in R package lsmeans [51]). For microbial diversity comparison, we used Wilcoxon rank-sum test with for Shannon index and PERMANOVA (Adonis function in R package vegan [52]) for beta diversity. Benjamin-Hochberg FDR (false discovery rate) correction was adopted for multiple

testing. Distance-based redundancy analysis (db-RDA) was conducted to identify the microbial variation contributed by the FMT and SOW effect using Bray Curtis dissimilarity distance. DESeq2 was adopted to identify differentially enriched microorganisms on the summarized species level and functional KEGG modules, and selected biomarkers were visualized in a heatmap by R package complexheatmap [53]. The correlation networks of microbial associations with clinical variables were calculated by Pearson's correlation analysis after centered log-ratio transformation, and the results were visualized by igraph and ggraph (R package).

For the MAG-level analysis, we adopted pairwise Wilcoxon rank-sum tests to determine statistical difference of MAG abundance and replication rate between groups, and the *p* values were adjusted by Benjamin-Hochberg FDR correction. Fisher's exact test was applied to identify differential presence of gene families and KEGG modules and between donor-specific strains and MAGs. Db-RDA was used to show functional dissimilarity of donor-specific MAGs (Bray Curtis distance based on KEGG module presence).

Results

Donor-dependent host response existed in recipient piglets

FMT from the Donor 2 significantly reduced the NEC incidence (CON vs. FMT2, 42 vs 0%, $p < 0.05$, Fig. 2A), whereas FMT from Donor 1 only resulted in a non-significant NEC reduction. The pathological severity of FMT2 piglets decreased across all gut segments (Additional file: Figure S3A), resulting in an overall reduction in pathological severity in FMT2 piglets relative to CON (Fig. 2B). Moreover, only FMT2 had reduced intestinal permeability as indicated by lower urinary lactulose-mannitol ratio relative to CON piglets (Fig. 2C). Furthermore, FMT2 piglets showed reduced diarrhea severity for the duration of the study (Additional file: Figure S3B) and had higher daily weight gain relative to FMT1 (Fig. 2D), while the digestive capacity of proteins (Fig. 2E) and carbohydrates (Fig. 2F) tended to be higher relative to CON. Gut histological evaluation showed no distinct change between treatment groups (Additional file: Figure S3C-S3F). However, linear regression analysis suggested that histological data was strongly related with NEC severity, where MPO score in colon and bacterial adhesion score explained most variance with R^2 values larger than 0.5 (Additional file: Figure S3G).

Fecal microbiota transplantation shifted the recipient gut microbiota in a donor-dependent manner

To determine GM changes induced by rectal FMT, we applied prokaryotic-specific 16S rRNA gene amplicon sequencing as well as broader profiling with shotgun metagenomics. The early-life GM of preterm pigs was dominated by *Bacteria*, containing more *Proteobacteria* but less *Bacteroidetes* when compared to the composition of both donors (Additional file: Figure S4A). The genus-level microbial composition of the two donors was quite similar (Additional file: Figure S4B and S3C), despite resulting in two distinct phenotypes in the recipients. All recipients including FMT2 piglets had lower microbial

Shannon diversity in the colon when compared to either of the two donors. However, the FMT2 group showed significantly higher gut microbial richness than FMT1 and CON (Fig. 3A and 3B). Both sequencing methods indicated that the GM of FMT2 piglets significantly differed from FMT1 and CON (Fig. 3C and 3D, Table 1). Donor and sow (maternal) effects were the two main independent factors affecting GM structure, which explained 15.4% and 6.4% of the total variance in the db-RDA model (Fig. 3E). NEC status explained only 5.8% and 4.1% of GM variation on unweighted UniFrac and binary Jaccard metrics, respectively profiled by amplicon sequencing and shotgun metagenomics (Additional file: Figure S5).

Table 1
Pairwise PERMANOVA between recipient groups on dissimilarity metrics.

	Weighed Unifac (16S rRNA[a])	**Unweighed Unifac (16S rRNA[a])**	**Bray Curtis (Shotgun species[b])**	**Binary Jaccard (Shotgun species[b])**	**Bray Curtis (Shotgun genus[c])**	**Binary Jaccard (Shotgun genus[c])**
FMT1 vs FMT2	R^2 = 0.093, *p*.adj = 0.092	R^2 = 0.099, *p*.adj = 0.007	R^2 = 0.13, *p*.adj = 0.0045	R^2 = 0.078, *p*.adj = 0.0045	R^2 = 0.15, *p*.adj = 0.01	R^2 = 0.075, *p*.adj = 0.01
FMT1 vs CON	R^2 = 0.045, *p*.adj = 0.3	R^2 = 0.23, *p*.adj = 0.0015	R^2 = 0.1, *p*.adj = 0.008	R^2 = 0.062, *p*.adj = 0.026	R^2 = 0.079, *p*.adj = 0.082	R^2 = 0.052, *p*.adj = 0.068
FMT2 vs CON	R^2 = 0.13, *p*.adj = 0.03	R^2 = 0.34, *p*.adj = 0.0015	R^2 = 0.23, *p*.adj = 0.003	R^2 = 0.13, *p*.adj = 0.003	R^2 = 0.24, *p*.adj = 0.003	R^2 = 0.12, *p*.adj = 0.003

[a]16S rRNA, dissimilarity metrics derived from 16S rRNA gene amplicons;

[b]Shotgun species, dissimilarity metrics derived from species-level profiling with Kaiju;

[c]Shotgun genus, dissimilarity metrics derived from genus-level profiling with Kaiju.

Enterobacteriaceae and *Enterococcaceae* dominated the neonatal GM of preterm piglets. Distinct increases in lactobacilli and *Streptococcus* were observed in the colon samples of both FMT groups relative to CON (Additional file: Figure S4C and S3D). Db-RDA analysis revealed that *Limosilactobacillus reuteri*, *Lactobacillus crispatus*, *Lactobacillus amylovorus* and *Streptococcus gallolyticus* contributed most of the variation induced by FMT (Fig. 3E). We adopted DESeq2 to identify species differentially abundant between treatment groups. Besides the prevalence of lactobacilli and *Streptococcus* spp., we found significant reductions in *Enterobacter cloacae*, *Staphylococcus aureus, Streptococcus orisratti*,

Clostridioides difficile and *Enterococcus faecium* in the gut of FMT2 piglets relative to CON (Fig. 4). In the colon samples of FMT1 piglets, we observed distinctly decreased abundance of *Lmb. reuteri*, *Lb. amylovorus*, *Ligilactobacillus agilis* and *Subdoligranulum variabile*, but more *Staph. aureus*, *E. faecium*, and *Strep. orisratti* (FMT1 vs FMT2, adjusted $p < 0.05$).

Engrafted lactobacilli strains differed according to the respective donors

The relative abundance of lactobacilli increased in colon samples of both FMT treatment groups, but also distinctly differed in between (Fig. 5A). *Lb. amylovorus*, *Lb. crispatus* and *Lmb. reuteri* were the predominantly detected lactobacilli species, and were found in the donors as well (Fig. 5B). The strains of *Lmb. reuteri* and *Lb. crispatus* in the recipients showed different donor sources when we aligned their phylogenetic marker genes (Fig. 5D). The functional difference of engrafted lactobacilli strains was compared using PanPhlAn, and 798 gene families for *Lmb. reuteri* and 432 for *Lb. crispatus* were found to be different between the strains from FMT1 and FMT2 piglets (Fisher's exact test, $p < 0.05$). These genes were associated with ABC transporters, fatty acid biosynthesis, amino acid biosynthesis/metabolism and drug resistance et al. (Additional file: Table S1 and S2)

Shifted gut microbiota composition was linked to gastrointestinal improvements

In addition to the donor-dependent changes in the recipient GM, the altered microbial composition was associated with gastrointestinal improvements by FMT. Using NEC, diarrhea severity and histological data as indicators of gastrointestinal health, we conducted Pearson's correlation analysis between the abundance of the core GM species and clinical variables. The abundances of *Cl. difficile*, *C. perfringens* and *E. faecium* positively correlated with NEC severity, MPO level and CD3 + cell density in the colon as well as bacterial adhesion score in the small intestine (Pearson's coefficient > 0.4). Although we did not detect a direct correlation between lactobacilli and NEC severity, the diarrhea severity negatively correlated with *Lmb. reuteri*, *Lgb. agilis* and *Subdo. variabile* relative abundance (Fig. 6).

Furthermore, the shifted microbial structure led to microbial communities of differential functional capacities. We established a non-redundant pig GM gene catalogue, annotated by the KEGG gene database. DESeq2 was adopted to identify differentially enriched KEGG modules between treatment groups (Figure S6). Compared with CON, the gut inhabitants in FMT2 piglets displayed distinct genetic enrichment involved in threonine (M00018), lysine (M00526, M00527) and acetate (M00579) biosynthesis. However, FMT1 piglets had less microbial genes encoding these functional capacities in colon but more genes associated staphlyloferrin B biosynthesis (M00875). Meanwhile, pathogenetic signatures from *Salmonella enterica* (M00856) and *Escherichia coli* (M00542) were detected in colon samples of FMT2 and FMT1 but rarely in that of CON (Additional file: Figure S6).

Genome-resolved analysis revealed donor-specific patterns in recipient piglets

To conduct the genome-resolved analysis between donors, we refined the output of four automatic binning tools (metabat2, maxbin2, concoct, vamb) and reconstructed in total 583 medium-quality MAGs including 394 high-quality ones (completeness > 90% and contamination < 5%). Different binning strategies were compared, and the subject-specific binning strategy generated more high-quality MAGs than binning on co-assemblies (Additional file: Figure S2). To mitigate mis-mapping bias caused by sequence homology, we used the breadth of coverage > 50% to determine the presence of a MAG in the donors. Under this criterion, piglets receiving FMT from the two donors had 199 shared MAGs, while 53 MAGs were unique to Donor 2 and 57 were unique to Donor 1. The bacterial replication rate was estimated by the sequencing coverage trend across the genome using iRep. Lactobacilli population displayed higher iRep values in the gut of FMT2 piglets relative to FMT1, and nearly none for CON (Fig. 7A). Among 309 MAGs present in donors, 74 MAGs showed differential relative abundance in the gut of FMT1 and FMT2 recipients (adjusted $p < 0.05$). Consistently with the mapping-based method, most of these MAGs belonged to lactobacilli and *Streptococcus* (Fig. 7B). The MAGs of *Lmb. reuteri, Lb. amylovorus* and *Subdo. variable* were mainly recovered in the colon samples from FMT2 piglets and Donor 2. *Lb. crispatus*, *Lmb. vaginalis* and *Strep. gallolyticus* were detected in both recipient groups but the MAGs differed according to their respective donors. Using the microbial markers provided by PhyloPhlAn, we assessed the phylogenetic relationship of the recovered MAGs. No donor-specific phylogenetic separation of the MAGs was found (Fig. 7C).

The functional similarity of donor-specific MAGs was compared based on the presence of KEGG modules in the genomes (Fig. 7D). The Donor 2-specific MAGs possessed more KEGG modules of heparan sulfate degradation (M00078, adjusted $p < 0.005$), keratan sulfate degradation (M00079, adjusted $p < 0.1$) and carbohydrate metabolism genes associated with the pentose phosphate pathway and galactose. Heparan and keratan sulfate are ubiquitous glycosaminoglycans (GAGs) in mammalian tissue. The two GAG-degradation modules were predominately harbored by *Bacteroides* e.g. *B. vulgatus* in Donor 2 (Breadth of coverage > 90%, Additional file: Table S4). The Donor 1-specific MAGs on the other hand showed functional enrichment in Staphyloferrin B biosynthesis and drug-resistant efflux pump QacA, which likely originated from *Staph. aureus* (Additional file: Table S3).

Discussion

FMT exhibits high cure rates (90% in average) when used to treat overgrowth of one specific pathogen, *Cl. difficile*, in the gut [54]. The success of FMT in rCDI treatment is not affected by a specific donor [55]. In a cohort compromising of 1999 FMT recipients and 28 donors, the rCDI cure rate was found to be high for all donors [54]. Encouraged by this overwhelming success, researchers have extended the use of FMT in a range of diseases characterized by GM dysbiosis e.g. IBD [56] and metabolic syndrome [57]. Contrarily, the super donor phenomenon appears to exist in FMT treatments of these diseases e.g. Crohn's disease [16], ulcerative colitis [17, 18], irritable bowel syndrome [19], type-2 diabetes [57]. Accordingly, we found NEC prevention among preterm piglet FMT recipients to be donor dependent. Recipients of the superior donor feces (FMT2) showed no NEC cases relative to 23% NEC incidence in recipients of the inferior

donor feces and 42% in the CON group. Moreover, FMT2 piglets exhibited improved gut function (e.g. barrier, digestion) and body weight gain.

A superior donor appears to be more essential for FMT use in multifactorial disease such as IBD and NEC, which result from complex interactions between host immune response, host genetics, GM, and exogenous intake e.g. formula feeding. Gut dysbiosis is implicated in the etiology and development of these diseases but none is considered to be solely induced by overgrowth of one specific microbe as rCDI. Given the existing redox potentials in gut [58], a preterm GM is usually characterized by relatively low microbial diversity and prolonged dominance of facultative anaerobes e.g. *Enterobacter*, *Enterococcus* and *Staphylococcus*, but delayed colonization by obligate anaerobes e.g. *Bifidobacterium* and *Bacteroides* [59]. This might provide favorable gastrointestinal condition of high NEC risk. Herein, we noticed that the donor-dependent phenomenon not only existed in the host response but also was reflected in the shifted recipient GM. Higher Shannon index and more lactobacilli but much less *Cl. difficile*, *C. perfringens* and *E. faecium* were found in the colon of FMT2 piglets receiving the superior donor feces.

Pathogen resistance is a noted advantage provided by GM [60], which is also expected to provide protection against NEC. Using Pearson's correlation analysis, we found the shifted abundance of *Cl. difficile* and *C. perfringens* and *E. faecium* positively linked with increased pathological severity and gut inflammation. Although we cannot causally link these species with NEC, we still note that efficient FMT may inhibit the colonization of opportunistic pathogens. Consistently, functional profiling of GM indicated the FMT2 group contained much less microbial genes encoding staphyloferrin synthesis, but more genes associated with lysine and acetate biosynthesis in the gut. Staphyloferrin is high-affinity siderophore excreted by *S. aureus* to acquire iron to proliferate [61]. This mechanism is employed by some pathogens to scavenge sequestrated iron from host and plays an essential role in bacterial virulence [62]. Reduction of these genetic elements suggested a declined risk of invasive gastroenteritis by *Staph. aureus*. Lysine, considered to be an essential amino acid, is found recently to be produced partially by GM and then absorbed by host [63]. GM-mediated amino acid metabolism could be essential for neonates given the high accretion of body protein. A disrupted GM, e.g. suppressed by antibiotics, is linked to decreased protein synthesis rate in gut [64]. Orally administrated lysine is also reported to ameliorate diarrhea symptoms in a rodent model [65]. Besides, the superior Donor 2 resulted in recipient GM with higher capacity for acetate production, which is in accordance with the reported increase of SCFA production using the same donor [20].

Donor species richness is reported to determine FMT success among IBD patients [16]. In this study, the two donor microbiotas had similar alpha diversity and composition but resulted in different alpha diversity, composition and clinical response after transplantation. Hence, microbial richness alone may not ensure the FMT efficiency. Our data suggest that even strain-level variation may play an important role and affect the bacterial engraftment. The two donors had comparable lactobacilli composition, however lactobacilli colonized recipients in a donor-dependent manner. Phylogenetic analysis indicated different strains of *Lmb. reuteri* and *Lb. crispatus* existed between the donors. Identified by PanPhlAn,

Lmb. reuteri strains from the superior donor (Donor 2) conferred more drug resistance genes such as colistin resistance protein EmrB. The strain-level variation likely made the *Lmb. reuteri* from Donor 2 more robust to cope with environmental challenges and led to a higher replication rate of lactobaclli in the gut. Besides, MAG-level analysis indicated that Donor 2 contained specific *Bacteroides* e.g. *B. vulgatus* conferring heparan and keratan sulfate utilization genes. Heparan and keratan sulfate are two major classes of GAGs on mammalian epithelial cells, which play a fundamental role in mutualistic bacteria adhesion [65, 66] as well as bacterial infectivity of pathogens. Given the high genome coverage of these MAGs solely in the superior donor, we suspected the GAG-degrading *Bacteriodes* might facilitate bacterial engraftment including lactobacilli and also competitively exclude other GAG-binding pathogens [68]. *Bacteroides* are considered as next-generation probiotics for their ubiquitous GAG-degrading capacity [66] and production of anti-inflammatory lipopolysaccharide [69]. Gavage of *B. vulgatus* is reported to alleviate murine endotoxemia by suppressing lipopolysaccharide production in gut [70]. One multi-donor FMT trial has also indicated that increased *Bacteroides* in donor stool is associated with ulcerative colitis remission in recipients [71].

Although rectal FMT showed promising properties in terms of preventing NEC, we also noticed increased pathogenetic signatures from *Escherichia coli* and *Salmonella enterica* in recipient guts. This highlights the risk of potential transmission of infectious agents during FMT, which also explains previously high sepsis cases through oral administration [20]. Even though the transferred enteropathogens did not violate the preventive effect of rectal FMT here, they might become a risk factor [72].

Conclusions

Rectal FMT manifested clinically and microbiologically in a donor-dependent manner, modulating gut dysbiosis of recipient preterm piglets and preventing NEC in a donor dependent manner. Strain-level difference of engrafted lactobacilli existed between donors. The donor with GAG-degrading *Bacteroides* exhibited superior microbial engraftment and provided superior pathogen resistance for recipients, which might constitute a promising direction for donor selection in future FMT treatment.

Abbreviations

FMT: Fecal microbiota transplantation

rCDI: Recurrent *Clostridioides difficile* infection

IBD: Inflammatory bowel disease

NEC: Necrotizing enterocolitis

GM: Gut microbiome

KEGG: Kyoto Encyclopedia of Genes and Genomes

MAG: Metagenomic assembly genome

FDR: False discovery rate

Db-RDA: Distance-based redundancy analysis

GAG: Glycosaminoglycan

MPO: Myeloperoxidase

LM: Lactulose mannitol

SI: Small intestine

DPPIV: Dipeptidyl peptidase IV

Declarations

Ethics approval and consent to participate

Not applicable.

Consent for publication

Not applicable.

Availability of data and materials

The raw sequence data of 16S rRNA gene amplicon sequencing and shotgun metagenomics were deposited in the Sequence Read Archive at NCBI under Bioproject PRJNA668104 (Reviewer link: https://dataview.ncbi.nlm.nih.gov/object/PRJNA668104?reviewer=gi8gtnqmm82nu26d4krifmtdh1). Codes for data analysis can be assessed on one public Github repository (https://github.com/yanhui09/FMT-donor).

Competing interests

The authors declare that they have no competing interests.

Funding

This study was financed by the Independent Research Fund Denmark under the project No. 8022-00188B, and Yan Hui was supported by China Scholarship Council under a PhD scholarship (No. 201706350028).

Author's contributions

Conceptualization: A.B., T.T. and D.S.N.; Investigations: Y.H., A.B. and L.D.; Methodology: A.B., Y.H., L.D., W.P.K. and G.V.; Project administration: A.B., T.T. and D.S.N.; Resources: A.B., T.T., W.P.K., D.S.N.; Supervision: T.T., G.V. and D.S.N.; Software: Y.H. and G.V.; Formal analysis: Y.H. and A.B.; Data curation: Y.H. and A.B.; Visualization: Y.H. and A.B.; Writing-original draft: Y.H. and A.B.; Writing-review and editing: all authors. Funding acquisitions: A.B., T.T. and D.S.N. All authors read and approved the final manuscript.

Acknowledgements

We want to acknowledge all laboratory technicians and experienced animal caretakers for their support in this study. We thank Professor Per Torp Sangild for his helpful suggestion. We also acknowledge the high-performance computing platform provided by Danish National Supercomputer for Life Sciences (Computerome, https://computerome.dtu.dk).

References

1. Neu J, Walker WA. Necrotizing Enterocolitis. N Engl J Med. 2011;364:255–64.
2. Alganabi M, Lee C, Bindi E, Li B, Pierro A. Recent advances in understanding necrotizing enterocolitis. F1000Research. 2019;8:107.
3. Obladen M. Necrotizing Enterocolitis – 150 Years of Fruitless Search for the Cause. Neonatology. 2009;96:203–10.
4. Jilling T, Simon D, Lu J, Meng FJ, Li D, Schy R, Thomson RB, Soliman A, Arditi M, Caplan MS. The Roles of Bacteria and TLR4 in Rat and Murine Models of Necrotizing Enterocolitis. J Immunol. 2006;177:3273–82.
5. Neal MD, Sodhi CP, Dyer M, Craig BT, Good M, Jia H, Yazji I, Afrazi A, Richardson WM, Beer-Stolz D, Ma C, Prindle T, Grant Z, Branca MF, Ozolek J, Hackam DJ. A Critical Role for TLR4 Induction of Autophagy in the Regulation of Enterocyte Migration and the Pathogenesis of Necrotizing Enterocolitis. J Immunol. 2013;190:3541–51.
6. Coggins SA, Wynn JL, Weitkamp J-H. Infectious Causes of Necrotizing Enterocolitis. Clin Perinatol. 2015;42:133–54.
7. De La Cochetière MF, Piloquet H, Des Robert C, Darmaun D, Galmiche JP, Rozé JC. Early intestinal bacterial colonization and necrotizing enterocolitis in premature infants: The putative role of Clostridium. Pediatr Res. 2004;56:366–70.

8. McMurtry VE, Gupta RW, Tran L, Blanchard EE, Penn D, Taylor CM, Ferris MJ. Bacterial diversity and Clostridia abundance decrease with increasing severity of necrotizing enterocolitis. Microbiome. 2015;3:1–8.
9. Pammi M, Cope J, Tarr PI, Warner BB, Morrow AL, Mai V, Gregory KE, Kroll JS, McMurtry V, Ferris MJ, Engstrand L, Lilja HE, Hollister EB, Versalovic J, Neu J. Intestinal dysbiosis in preterm infants preceding necrotizing enterocolitis: a systematic review and meta-analysis. Microbiome. 2017;5:31.
10. Olm MR, Bhattacharya N, Crits-Christoph A, Firek BA, Baker R, Song YS, Morowitz MJ, Banfield JF. Necrotizing enterocolitis is preceded by increased gut bacterial replication, *Klebsiella*, and fimbriae-encoding bacteria. Sci Adv. 2019;5:eaax5727.
11. Bury RG, Tudehope D. Enteral antibiotics for preventing necrotising enterocolitis in low birthweight or preterm infants. Cochrane database Syst Rev. 2000;2001:CD000405.
12. Sharif S, Meader N, Oddie SJ, Rojas-Reyes MX, McGuire W. Probiotics to prevent necrotising enterocolitis in very preterm or very low birth weight infants. Cochrane Database Syst Rev. 2020;10:CD005496.
13. Lin PW, Stoll BJ. Necrotising enterocolitis. Lancet. 2006;368:1271–83.
14. Cui B, Li P, Xu L, Peng Z, Xiang J, He Z, Zhang T, Ji G, Nie Y, Wu K, Fan D, Zhang F. Step-up fecal microbiota transplantation (FMT) strategy. Gut Microbes. 2016;7:323–8.
15. Wilson BC, Vatanen T, Cutfield WS, O'Sullivan JM. The super-donor phenomenon in fecal microbiota transplantation. Front Cell Infect Microbiol. 2019;9:2.
16. Vermeire S, Joossens M, Verbeke K, Wang J, Machiels K, Sabino J, Ferrante M, Van Assche G, Rutgeerts P, Raes J. Donor Species Richness Determines Faecal Microbiota Transplantation Success in Inflammatory Bowel Disease. J Crohn's Colitis. 2016;10:387–94.
17. Moayyedi P, Surette MG, Kim PT, Libertucci J, Wolfe M, Onischi C, Armstrong D, Marshall JK, Kassam Z, Reinisch W, Lee CH. Fecal Microbiota Transplantation Induces Remission in Patients With Active Ulcerative Colitis in a Randomized Controlled Trial. Gastroenterology. 2015;149:102–9.e6.
18. Paramsothy S, Kamm MA, Kaakoush NO, Walsh AJ, van den Bogaerde J, Samuel D, Leong RWL, Connor S, Ng W, Paramsothy R, Xuan W, Lin E, Mitchell HM, Borody TJ. Multidonor intensive faecal microbiota transplantation for active ulcerative colitis: a randomised placebo-controlled trial. Lancet. 2017;389:1218–28.
19. Mizuno S, Masaoka T, Naganuma M, Kishimoto T, Kitazawa M, Kurokawa S, Nakashima M, Takeshita K, Suda W, Mimura M, Hattori M, Kanai T. Bifidobacterium-Rich Fecal Donor May Be a Positive Predictor for Successful Fecal Microbiota Transplantation in Patients with Irritable Bowel Syndrome. Digestion. 2017;96:29–38.
20. Brunse A, Martin L, Rasmussen TS, Christensen L, Skovsted Cilieborg M, Wiese M, Khakimov B, Pieper R, Nielsen DS, Sangild PT, Thymann T. Effect of fecal microbiota transplantation route of administration on gut colonization and host response in preterm pigs. ISME J. 2019;13:720–33.
21. Sangild PT, Siggers RH, Schmidt M, Elnif J, Bjornvad CR, Thymann T, Grondahl ML, Hansen AK, Jensen SK, Boye M, Moelbak L, Buddington RK, Weström BR, Holst JJ, Burrin DG. Diet- and

Colonization-Dependent Intestinal Dysfunction Predisposes to Necrotizing Enterocolitis in Preterm Pigs. Gastroenterology. 2006;130:1776–92.

22. Sangild PT, Thymann T, Schmidt M, Stoll B, Burrin DG, Buddington RK. Invited Review: The preterm pig as a model in pediatric gastroenterology. J Anim Sci. 2013;91:4713–29.
23. Østergaard MV, Shen RL, Støy ACF, Skovgaard K, Krych Ł, Leth SS, Nielsen DS, Hartmann B, Bering SB, Schmidt M, Sangild PT. Provision of Amniotic Fluid During Parenteral Nutrition Increases Weight Gain With Limited Effects on Gut Structure, Function, Immunity, and Microbiology in Newborn Preterm Pigs. J Parenter Enter Nutr. 2016;40:552–66.
24. Krych Ł, Kot W, Bendtsen KMB, Hansen AK, Vogensen FK, Nielsen DS. Have you tried spermine? A rapid and cost-effective method to eliminate dextran sodium sulfate inhibition of PCR and RT-PCR. J Microbiol Methods. 2018;144:1–7.
25. Ren S, Hui Y, Goericke-Pesch S, Pankratova S, Kot W, Pan X, Thymann T, Sangild PT, Nguyen DN. Gut and immune effects of bioactive milk factors in preterm pigs exposed to prenatal inflammation. Am J Physiol Liver Physiol. 2019;317:G67–77.
26. Rognes T, Flouri T, Nichols B, Quince C, Mahé F. VSEARCH: a versatile open source tool for metagenomics. PeerJ. 2016;4:e2584.
27. McMurdie PJ, Holmes S. phyloseq: An R Package for Reproducible Interactive Analysis and Graphics of Microbiome Census Data. PLoS One. 2013;8:e61217.
28. Zheng J, Wittouck S, Salvetti E, Franz CMAP, Harris HMB, Mattarelli P, O'Toole PW, Pot B, Vandamme P, Walter J, Watanabe K, Wuyts S, Felis GE, Gänzle MG, Lebeer S. A taxonomic note on the genus Lactobacillus: Description of 23 novel genera, emended description of the genus Lactobacillus Beijerinck 1901, and union of Lactobacillaceae and Leuconostocaceae. Int J Syst Evol Microbiol. 2020;70:2782–858.
29. Tange O. GNU Parallel: the command-line power tool.;login USENIX Mag. 2011.
30. Uritskiy GV, Diruggiero J, Taylor J. MetaWRAP - A flexible pipeline for genome-resolved metagenomic data analysis 08 Information and Computing Sciences 0803 Computer Software 08 Information and Computing Sciences 0806 Information Systems. Microbiome. 2018;6:158.
31. Menzel P, Ng KL, Krogh A. Fast and sensitive taxonomic classification for metagenomics with Kaiju. Nat Commun. 2016;7:11257.
32. Nurk S, Meleshko D, Korobeynikov A, Pevzner PA. metaSPAdes: a new versatile metagenomic assembler. Genome Res. 2017;27:824–34.
33. Zhu W, Lomsadze A, Borodovsky M. Ab initio gene identification in metagenomic sequences. Nucleic Acids Res. 2010;38:e132–2.
34. Steinegger M, Söding J. Clustering huge protein sequence sets in linear time. Nat Commun. 2018;9:1–8.
35. Shen W, Le S, Li Y, Hu F. SeqKit: A Cross-Platform and Ultrafast Toolkit for FASTA/Q File Manipulation. PLoS One. 2016;11:e0163962.

36. Kanehisa M, Sato Y, Morishima K. BlastKOALA and GhostKOALA: KEGG Tools for Functional Characterization of Genome and Metagenome Sequences. J Mol Biol. 2016;428:726–31.
37. Li H. Aligning sequence reads, clone sequences and assembly contigs with BWA-MEM. Published Online First: 2013.http://arxiv.org/abs/1303.3997.
38. Li H, Handsaker B, Wysoker A, Fennell T, Ruan J, Homer N, Marth G, Abecasis G, Durbin R, Project G, Subgroup DP. The Sequence Alignment/Map format and SAMtools. Bioinforma Appl NOTE. 2009;25:2078–9.
39. Olm MR, Brown CT, Brooks B, Banfield JF. dRep: a tool for fast and accurate genomic comparisons that enables improved genome recovery from metagenomes through de-replication. ISME J. 2017;11:2864–8.
40. Pasolli E, Asnicar F, Manara S, Zolfo M, Karcher N, Armanini F, Beghini F, Manghi P, Tett A, Ghensi P, Collado MC, Rice BL, DuLong C, Morgan XC, Golden CD, Quince C, Huttenhower C, Segata N. Extensive Unexplored Human Microbiome Diversity Revealed by Over 150,000 Genomes from Metagenomes Spanning Age, Geography, and Lifestyle. Cell. 2019;176:649–62.e20.
41. Nissen JN, Sonderby CK, Armenteros JJA, Groenbech CH, Nielsen HB, Petersen TN, Winther O, Rasmussen S. Binning microbial genomes using deep learning. bioRxiv. 2018;:490078.
42. Hyatt D, Chen G-L, LoCascio PF, Land ML, Larimer FW, Hauser LJ. Prodigal: prokaryotic gene recognition and translation initiation site identification. BMC Bioinformatics. 2010;11:119.
43. CoverM. Read coverage calculator for metagenomics. https://github.com/wwood/CoverM.
44. Stewart RD, Auffret MD, Snelling TJ, Roehe R, Watson M. MAGpy: a reproducible pipeline for the downstream analysis of metagenome-assembled genomes (MAGs). Bioinformatics. 2019;35:2150–2.
45. Brown CT, Olm MR, Thomas BC, Banfield JF. Measurement of bacterial replication rates in microbial communities. Nat Biotechnol. 2016;34:1256–63.
46. Truong DT, Tett A, Pasolli E, Huttenhower C, Segata N. Microbial strain-level population structure and genetic diversity from metagenomes. Genome Res. 2017;27:626–38.
47. Scholz M, Ward DV, Pasolli E, Tolio T, Zolfo M, Asnicar F, Truong DT, Tett A, Morrow AL, Segata N. Strain-level microbial epidemiology and population genomics from shotgun metagenomics. Nat Methods. 2016;13:435–8.
48. Seemann T. Prokka: rapid prokaryotic genome annotation. Bioinformatics. 2014;30:2068–9.
49. Wickham H. *ggplot2: Elegant Graphics for Data Analysis Using the Grammar of Graphics*. 2016. https://ggplot2.tidyverse.org.
50. Bates D, Mächler M, Bolker B, Walker S. Fitting Linear Mixed-Effects Models Using lme4. J Stat Softw. 2015;67. doi:10.18637/jss.v067.i01.
51. Lenth RV. Using lsmeans. J Stat Softw. 2016.
52. Dixon P. VEGAN, a package of R functions for community ecology. J Veg Sci. 2003;14:927–30.

53. Gu Z, Eils R, Schlesner M. Complex heatmaps reveal patterns and correlations in multidimensional genomic data. Bioinformatics. 2016;32:2847–9.
54. Osman M, Stoltzner Z, O'Brien K, Ling K, Koelsch E, Dubois N, Amaratunga K, Smith M, Kassam Z. Donor Efficacy in Fecal Microbiota Transplantation for Recurrent Clostridium difficile: Evidence From a 1,999-Patient Cohort. Open Forum Infect Dis. 2016;3. doi:10.1093/ofid/ofw194.48.
55. Kassam Z, Lee CH, Yuan Y, Hunt RH. Fecal Microbiota Transplantation for Clostridium difficile Infection: Systematic Review and Meta-Analysis. Am J Gastroenterol. 2013;108:500–8.
56. Paramsothy S, Paramsothy R, Rubin DT, Kamm MA, Kaakoush NO, Mitchell HM. Castaño-Rodríguez N. Faecal Microbiota Transplantation for Inflammatory Bowel Disease: A Systematic Review and Meta-analysis. J Crohn's Colitis. 2017;11:1180–99.
57. Vrieze A, Van Nood E, Holleman F, Salojärvi J, Kootte RS, Bartelsman JFWM, Dallinga-Thie GM, Ackermans MT, Serlie MJ, Oozeer R, Derrien M, Druesne A, Van Hylckama Vlieg JET, Bloks VW, Groen AK, Heilig HGHJ, Zoetendal EG, Stroes ES, De Vos WM, Hoekstra JBL, Nieuwdorp M. Transfer of intestinal microbiota from lean donors increases insulin sensitivity in individuals with metabolic syndrome. Gastroenterology. 2012;143:913–6.e7.
58. Penders J, Thijs C, Vink C, Stelma FF, Snijders B, Kummeling I, van den Brandt PA, Stobberingh EE. Factors Influencing the Composition of the Intestinal Microbiota in Early Infancy. Pediatrics. 2006;118:511–21.
59. Henderickx JGE, Zwittink RD, van Lingen RA, Knol J, Belzer C. The Preterm Gut Microbiota: An Inconspicuous Challenge in Nutritional Neonatal Care. Front Cell Infect Microbiol. 2019;9:85.
60. McLaren MR, Callahan BJ. Pathogen resistance may be the principal evolutionary advantage provided by the microbiome. Philos Trans R Soc B Biol Sci. 2020;375:20190592.
61. Hammer ND, Skaar EP. Molecular Mechanisms of Staphylococcus aureus Iron Acquisition. Annu Rev Microbiol. 2011;65:129–47.
62. Parrow NL, Fleming RE, Minnick MF. Sequestration and Scavenging of Iron in Infection. Infect Immun. 2013;81:3503–14.
63. Metges CC, Eberhard M, Petzke KJ. Synthesis and absorption of intestinal microbial lysine in humans and non-ruminant animals and impact on human estimated average requirement of dietary lysine. Curr Opin Clin Nutr Metab Care. 2006;9:37–41.
64. Puiman P, Stoll B, Mølbak L, de Bruijn A, Schierbeek H, Boye M, Boehm G, Renes I, van Goudoever J, Burrin D. Modulation of the gut microbiota with antibiotic treatment suppresses whole body urea production in neonatal pigs. Am J Physiol Liver Physiol. 2013;304:G300–10.
65. Smriga M, Torii K. L-Lysine acts like a partial serotonin receptor 4 antagonist and inhibits serotonin-mediated intestinal pathologies and anxiety in rats. Proc Natl Acad Sci. 2003;100:15370–5.
66. Kawai K, Kamochi R, Oiki S, Murata K, Hashimoto W. Probiotics in human gut microbiota can degrade host glycosaminoglycans. Sci Rep. 2018;8:10674.
67. Martín R, Martín C, Escobedo S, Suárez JE, Quirós LM. Surface glycosaminoglycans mediate adherence between HeLa cells and Lactobacillus salivarius Lv72. BMC Microbiol. 2013;13:210.

68. Menozzi FD, Pethe K, Bifani P, Soncin F, Brennan MJ, Locht C. Enhanced bacterial virulence through exploitation of host glycosaminoglycans. Mol Microbiol. 2002;43:1379–86.
69. Steimle A, Michaelis L, Di Lorenzo F, Kliem T, Münzner T, Maerz JK, Schäfer A, Lange A, Parusel R, Gronbach K, Fuchs K, Silipo A, Öz HH, Pichler BJ, Autenrieth IB, Molinaro A, Frick J-S. Weak Agonistic LPS Restores Intestinal Immune Homeostasis. Mol Ther. 2019;27:1974–91.
70. Yoshida N, Emoto T, Yamashita T, Watanabe H, Hayashi T, Tabata T, Hoshi N, Hatano N, Ozawa G, Sasaki N, Mizoguchi T, Amin HZ, Hirota Y, Ogawa W, Yamada T, Hirata KI. Bacteroides vulgatus and Bacteroides dorei Reduce Gut Microbial Lipopolysaccharide Production and Inhibit Atherosclerosis. Circulation. 2018;138:2486–98.
71. Paramsothy S, Nielsen S, Kamm MA, Deshpande NP, Faith JJ, Clemente JC, Paramsothy R, Walsh AJ, van den Bogaerde J, Samuel D, Leong RWL, Connor S, Ng W, Lin E, Borody TJ, Wilkins MR, Colombel J-F, Mitchell HM, Kaakoush NO. Specific Bacteria and Metabolites Associated With Response to Fecal Microbiota Transplantation in Patients With Ulcerative Colitis. Gastroenterology. 2019;156:1440–54.e2.
72. Ward DV, Scholz M, Zolfo M, Taft DH, Schibler KR, Tett A, Segata N, Morrow AL. Metagenomic Sequencing with Strain-Level Resolution Implicates Uropathogenic E. coli in Necrotizing Enterocolitis and Mortality in Preterm Infants. Cell Rep. 2016;14:2912–24.

Figures

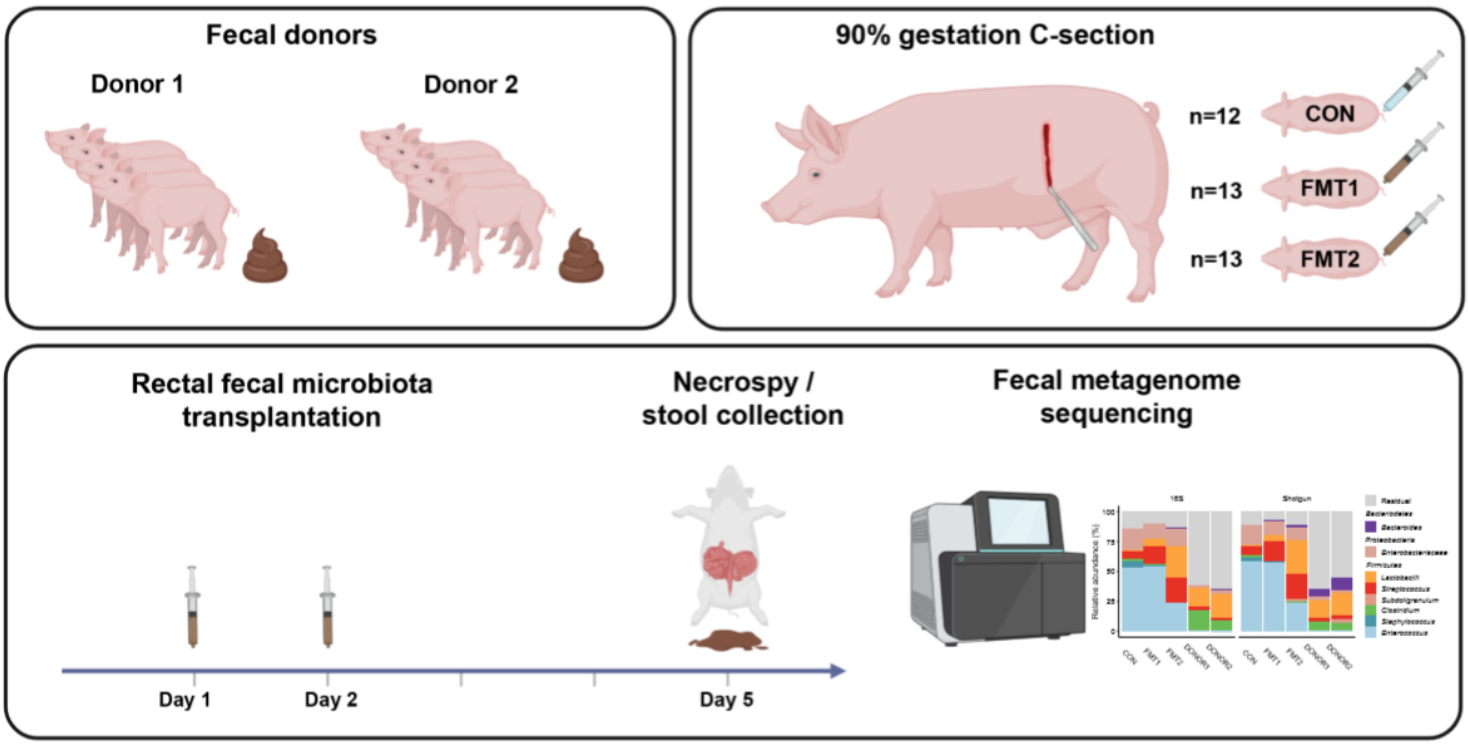

Figure 1

Study design. Respectively n= 13, 13, 12 for FMT1, FMT2 and CON. FMT1, rectal FMT with Donor 1; FMT2, rectal FMT with Donor 2; CON, rectal FMT with sterile saline as control.

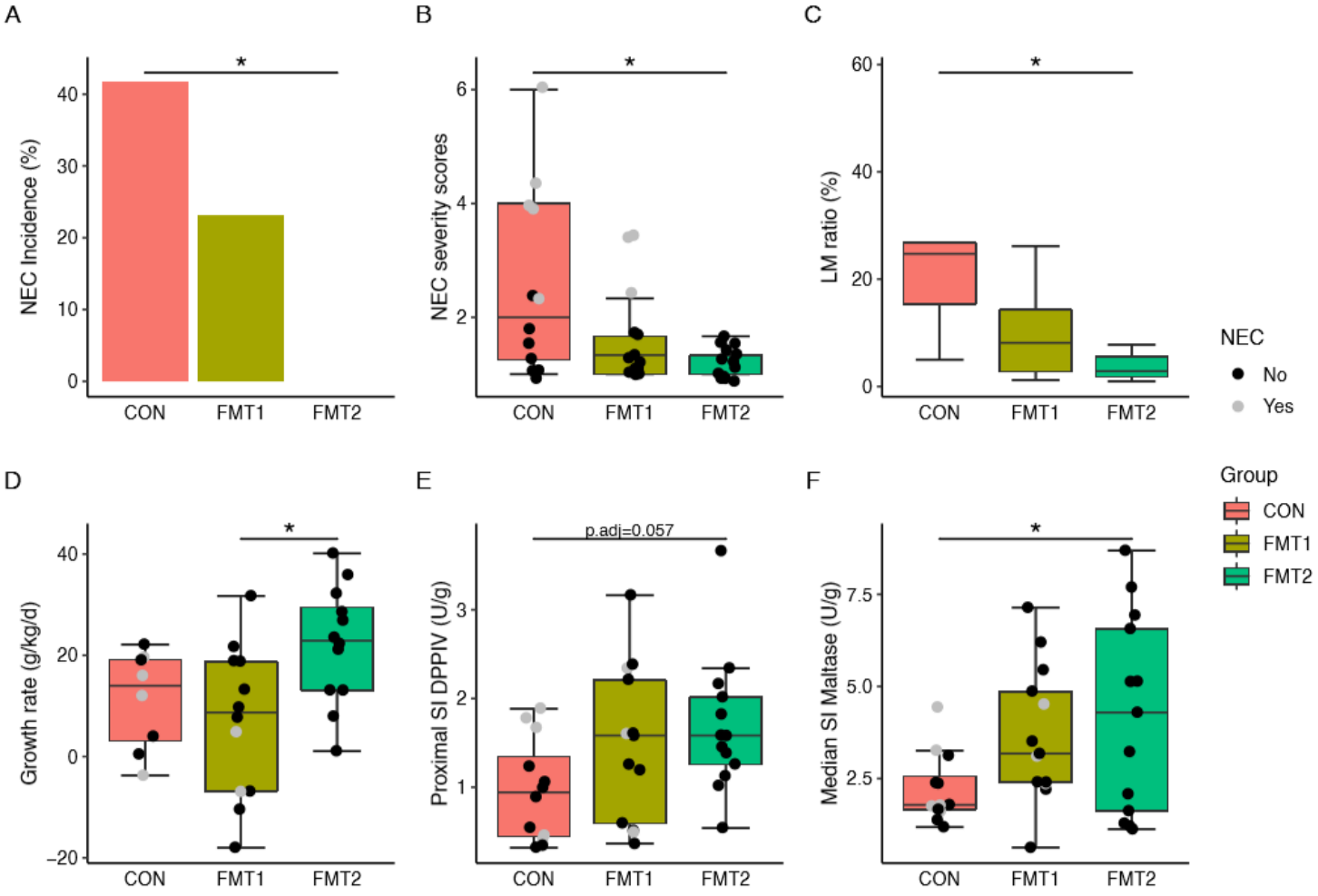

Figure 2

Donor-dependent host response existed in recipient piglets. FMT2 piglets showed superior survival and development status with lower NEC incidence (A) and necrosis severity (B) and improved gut barrier (C), daily weight gain (D) and digestive enzyme excretion (E, F). The labels of * represent adjusted $p < 0.05$. Except LM ratio and growth rate, n= 13, 13, 12 respectively for FMT1, FMT2 and CON. For LM ratios, respectively n = 8, 8, 5 while n = 12, 12, 8 for growth rate. FMT1, rectal FMT with Donor 1; FMT2, rectal FMT with Donor 2; CON, rectal FMT with sterile saline as control; NEC, necrotizing enterocolitis; LM ratio, urinary lactulose-mannitol ratio; SI DPPIV, dipeptidyl peptidase IV activity in small intestine; SI Maltase, maltase activity in small intestine.

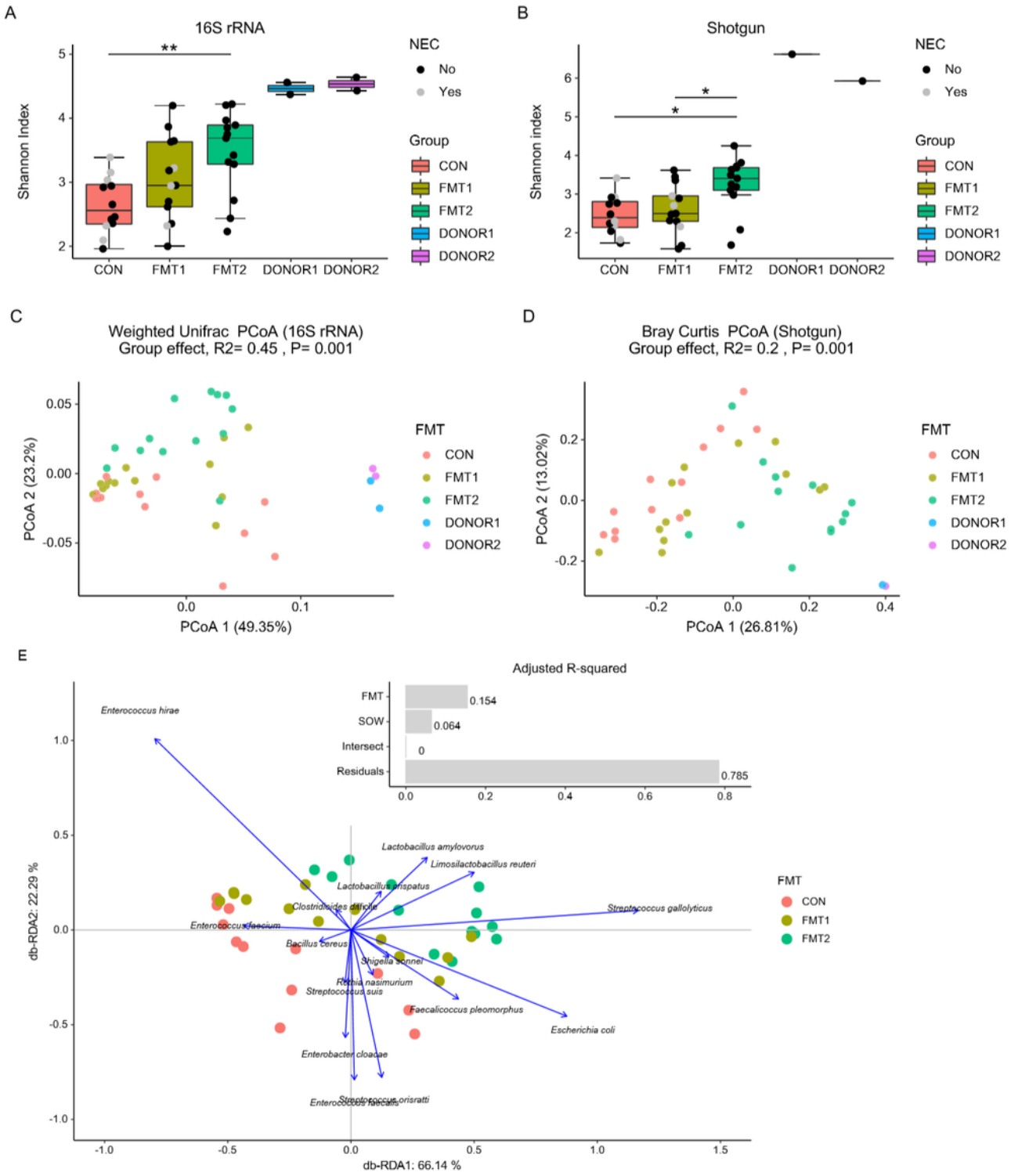

Figure 3

FMT shifted the recipient gut microbiota in a donor-dependent manner. Shannon index calculated from 16S rRNA gene amplicon sequencing (A) and Shotgun metagenomics (B); Unsupervised PCoA plots based on weighted UniFrac (C) and Bray Curtis dissimilarity metrics (D), and the db-RDA biplot showing the variance explained by FMT and SOW and the scaled loadings of core species (mean relative abundance > 1%) (E). Respectively n= 13, 13, 12 for FMT1, FMT2 and CON. FMT1, rectal FMT with Donor

1; FMT2, rectal FMT with Donor 2; CON, rectal FMT with sterile saline as control; NEC, necrotizing enterocolitis; 16S rRNA, 16S ribosome RNA gene amplicon sequencing; Shotgun, Shotgun metagenomics.

Figure 4

Differentially abundant taxa in colon between recipient groups. Differentially abundant core species (relative abundance > 1% among at least the 10% of samples) is shown under the cutoff of adjusted p < 0.05. Respectively n= 13, 13, 12 for FMT1, FMT2 and CON. FMT1, rectal FMT with Donor 1; FMT2, rectal FMT with Donor 2; CON, rectal FMT with sterile saline as control; GM, gut microbiome; NEC, necrotizing enterocolitis.

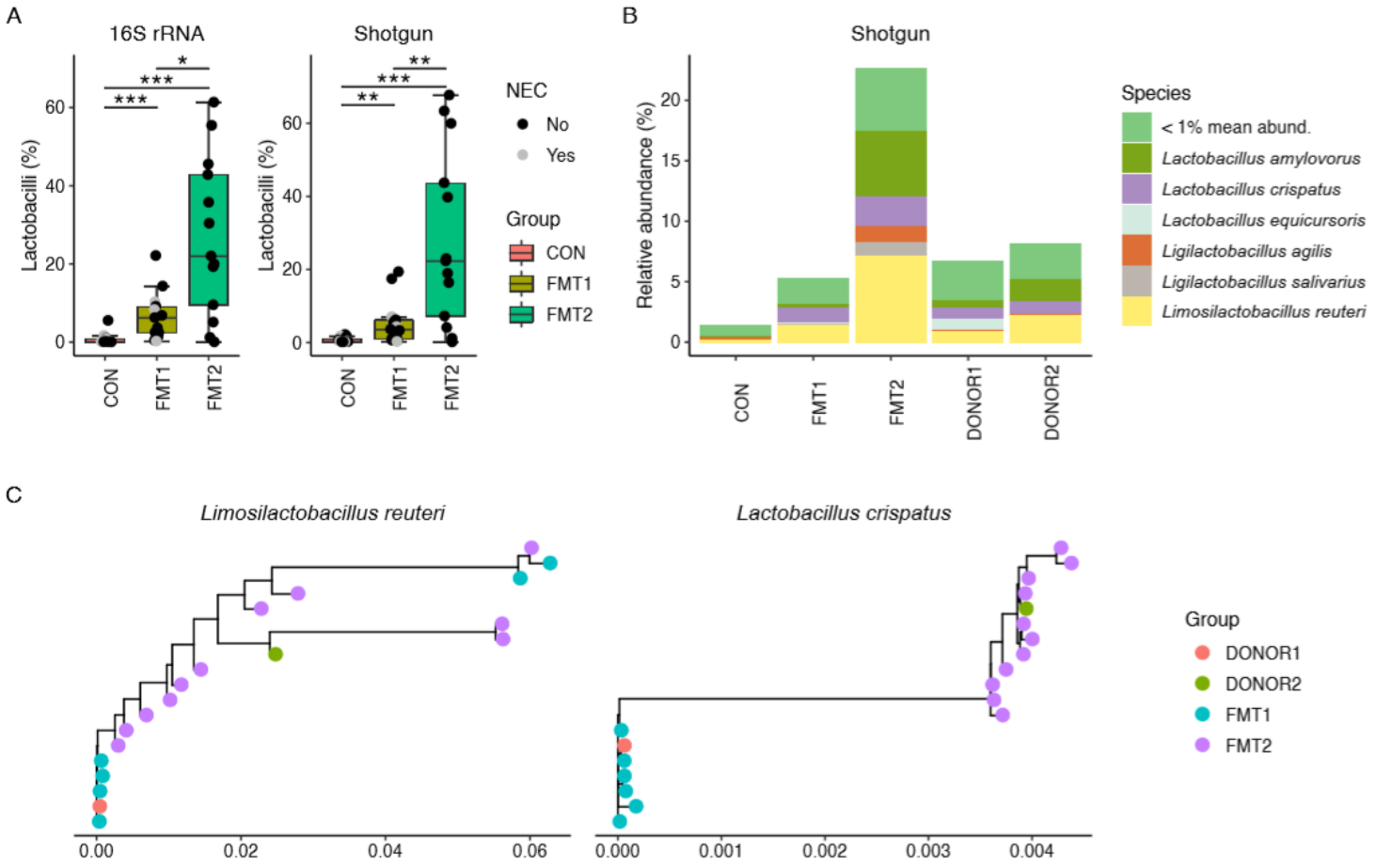

Figure 5

Engrafted lactobacilli strains differed according to the respective donors. The relative abundance (A) and dominant species (B) of lactobacilli, and strain tracking of Lmb. reuteri and Lb. crispatus by StrainPhlAn (C). Lactobacilli with minimum mean relative abundance of 1% are shown. Respectively n= 13, 13, 12 for FMT1, FMT2 and CON. FMT1, rectal FMT with Donor 1; FMT2, rectal FMT with Donor 2; CON, rectal FMT with sterile saline as control; 16S rRNA, 16S ribosome RNA amplicon sequencing; Shotgun, Shotgun metagenomics.

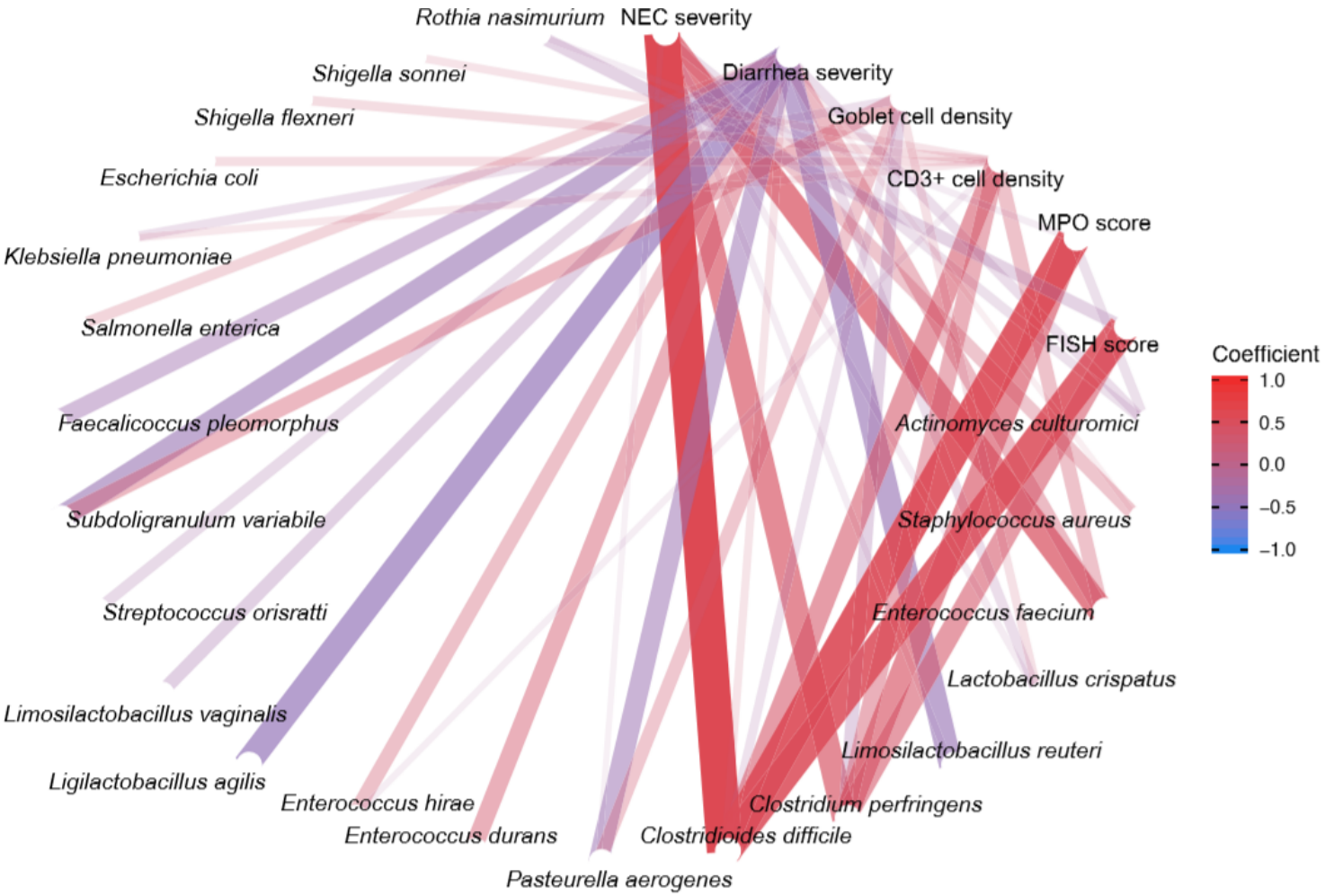

Figure 6

Shifted gut microbiota composition was linked to gastrointestinal improvements. Core microbiome is used for correlation analysis (relative abundance > 1% among at least the 10% of samples). The average NEC and diarrhea severity are taken as the indicators for gastrointestinal health, together with histological evaluation including goblet cell density, CD3+ cell density and MPO score in colon and FISH score in small intestine. The correlations are shown with absolute values of coefficients higher than 0.2. GM, gut microbiome; NEC, necrotizing enterocolitis; MPO, myeloperoxidase.

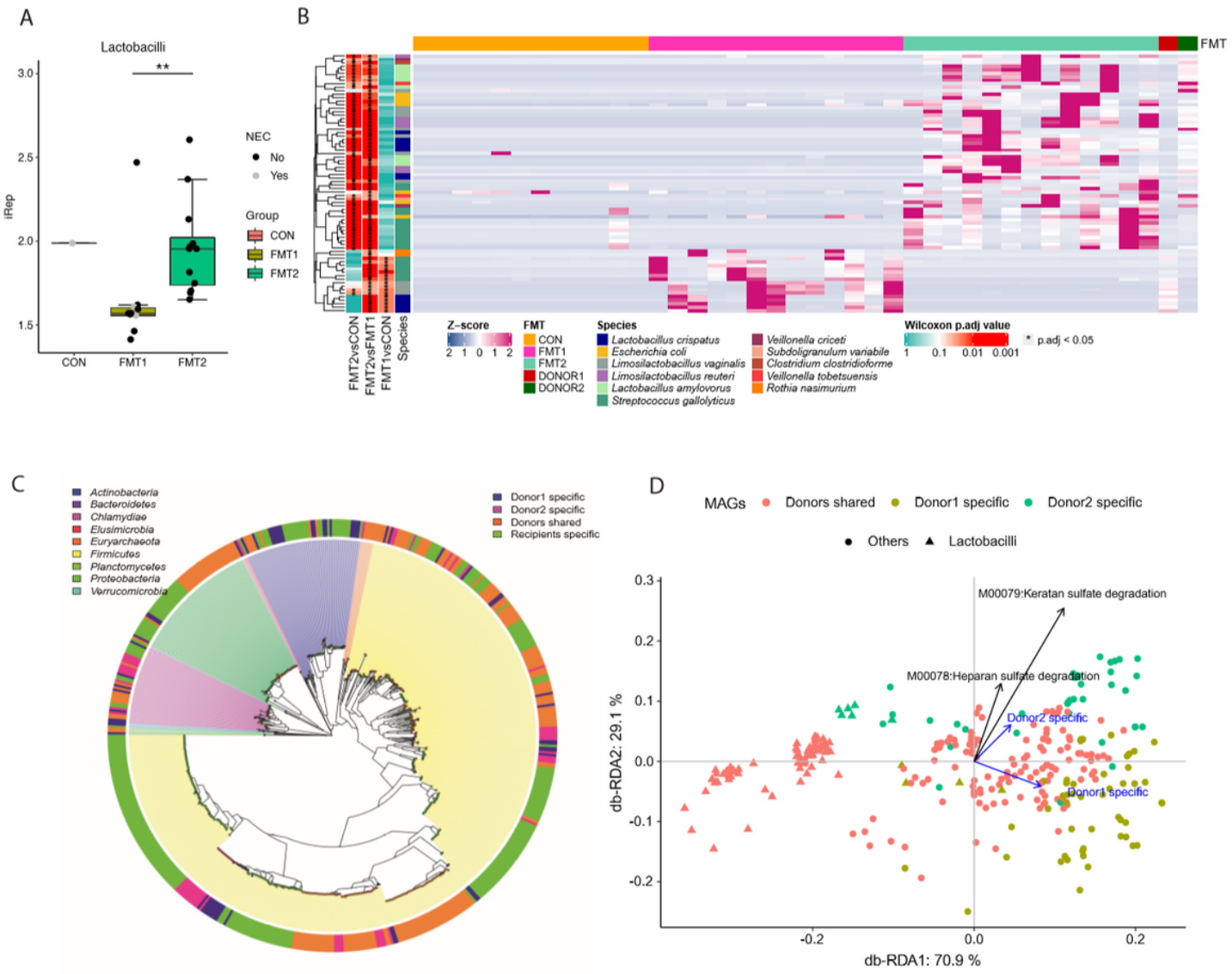

Figure 7

Shifted gut microbiota composition was linked to gastrointestinal improvements. Core microbiome is used for correlation analysis (relative abundance > 1% among at least the 10% of samples). The average NEC and diarrhea severity are taken as the indicators for gastrointestinal health, together with histological evaluation including goblet cell density, CD3+ cell density and MPO score in colon and FISH score in small intestine. The correlations are shown with absolute values of coefficients higher than 0.2. GM, gut microbiome; NEC, necrotizing enterocolitis; MPO, myeloperoxidase.

Supplementary Files

This is a list of supplementary files associated with this preprint. Click to download.

- SupplementaryTable.xlsx

- figureS1.pdf
- figureS2.pdf
- figureS3.pdf
- figureS4.pdf
- figureS5.pdf
- figureS6.pdf